Results in Nonlinear Analysis 8 (2025) No. 3, 1–14 https://doi.org/10.31838/rna/2025.08.03.001 Available online at www.nonlinear-analysis.com



# Results in Nonlinear Analysis

Peer Reviewed Scientific Journal

# An information analysis of a novel fractional chaotic systems and its application to image encryption

Adil Khudhair Bagheedh, Uday Jabbar Quaez, Mohammed J. Fari

Department of Mathematics, Mustansiriyah of University, Baghdad, Iraq.

#### Abstract

This paper introduces a new class of fractional chaotic systems with no fixed points, corresponding to standard chaotic maps, which exhibit chaotic behavior. We show the relationships between entropy in information theory and intrinsic properties in chaos theory of the proposed system. The chaotic behavior of this class is analyzed by exploring numerically using phase plots, bifurcation diagrams, Lyapunov exponents, and approximate entropy to examine the dynamics of the designed system and assess the effectiveness of varying the fractional order. An exact expression for solutions of the system is determined. Additionally, a new chaotic attractor is presented. In the practical aspect of this work, we present an image encryption algorithm based on the proposed system. Based on the experimental results obtained, we can conclude that the proposed algorithm achieves effective encryption with enhanced security, making it resistant to common attacks.

Mathematics Subject Classification (2010): 37D45, 37N20, 94A17, 94A60

Key words and phrases: Approximate entropy Chaotic behaviour Lyapunov exponents Image encryption.

### 1. Introduction

Both types, discrete and continuous fractional dynamical systems, have recently proved to be exciting, fruitful, and valuable tools in the modeling of many applications in different fields, such as Electrical, speech processing, Electronics, biological signal, Computer Engineering, and communication

Email addresses: aaddeel83@uomustansiriyah.edu.iq (Adil Bagheedh), dr.uday@uomustansiriyah.edu.iq (Uday Quaez), mohmmed.j82@uomustansiriyah.edu.iq (Mohammed Fari)

systems, etc. [1-4, 26]. Over the years, many studies of different chaotic systems have been introduced in various fields [5–11]. In a notable study [12], the authors explored the dynamic characteristics of a fractional-order chaotic system, corresponding to a classical system known for its chaotic behavior. The investigation delves into the intricate differences and properties that emerge when transitioning from standard to fractional-order systems, providing valuable insights into the nature of chaos in fractional dynamics [13] proposed a fractional chaotic system based on the integer order standard system. They analyzed the chaotic behavior of their proposed system by using bifurcation diagrams and experimental bounds on the placement of fractional order. [14] designed a continuous fractional chaotic system from the discrete logistic map by using a new technique based on delay time. The analysis and control of dynamical systems have been extensively studied in the literature, investigated [4, 15, 16]. It has been frequently asserted that chaotic trajectories exhibit aperiodic behavior, closely resembling random processes [17]. The loss of information is characterized by the flow of information about the initial state by the evolution of a conditional Shannon entropy, which generalizes the KS entropy for the case of observing the uncertainty more than one step ahead into the future [18]. Our work is interested in examining the dynamics of proposed fractional chaotic systems from the perspective of information theory. It is well known that dynamical systems without fixed points do not possess equilibrium states that can be analyzed for stability. Instead, chaos emerges directly from the system's intrinsic dynamics. This distinctive feature enhances their cryptographic performance, as they are associated with higher degrees of chaotic behavior compared to conventional systems. Consequently, these systems are considered more suitable for applications in secure communication and encryption.

The approximate entropy can be considered as a measure to determine the chaotic range of dynamical systems. Consequently, we use this measure to discuss the chaotic behavior of fraction dynamical systems in discrete time. We show that fractal orders have a significant and noticeable effect on the chaotic behavior of study systems; therefore, they can be considered as a key player in that. Furthermore, a novel image encryption algorithm based on the proposed chaotic system has been introduced. Experimental analyses conducted on a diverse set of images demonstrate that the proposed algorithm not only achieves a high level of encryption effectiveness but also exhibits exceptional robustness, making it highly resistant to cryptographic attacks. As a result, it significantly enhances overall security. The obtained results are favorable when compared to previous studies, showcasing clear improvements in both security and performance.

## 2. Preliminaries

 $N_{\tau}$  denotes the isolated time scale,  $N_{\tau} = \{\tau, \tau + 1, \tau + 2, ...\}, (\tau \in R \text{ fixed}).$ 

**Definition 2.1** [19] If  $g: N_{\tau} \to R$  and  $\delta > 0$  ( $\delta$  dosent belong to nutural numbers), then  $\delta$  – fractional difference operator is

$$\Delta^{p} g(t) = \Delta^{p-1} g(t+1) - \Delta^{p-1} \Phi(t)$$
(1)

And  $\Delta^0 g(t) = g(t)$ . This gives,

$$\Delta^{p} g(t) = \sum_{k=0}^{p} (-1)^{k} C_{k}^{p} \Delta^{p-1} g(t+p-k)$$
(2)

**Definition 2.2** [20] If  $g: N_{\tau} \to R$  and  $\delta > 0$  ( $\delta$  dosent belong to nutural numbers), then  $\delta$  – fractional difference operator is

$$\Delta_{\tau}^{\delta} g(t) = \frac{1}{\Gamma(\delta)} \sum_{s=\tau}^{t-\delta} (t - \Phi(s))^{(\delta-1)} g(s) , \quad t \in N_{\tau+\delta}$$
(3)

Here,  $\tau$  represents the initial point, while  $\Phi(s)$  is defined as  $\Phi(s) = s + 1$ . The term  $t^{\delta}$  refers to the falling function, mathematically expressed as  $t^{(\delta)} = \frac{\Gamma(t+1)}{\Gamma(t+1-\delta)}$  where  $\Gamma$  denotes the Gamma function.

**Definition 2.3** [20] For any  $\delta > 0$  and for a function g(t) defined on  $N_{\tau}$ , the Caputo like delta difference of order  $\delta$  is defined as follows

$${}^{C}\Delta_{\tau}^{\delta}g\left(t\right) = \frac{1}{\Gamma\left(p-\delta\right)} \sum_{s=\tau}^{t-(p-\delta)} \left(t-\Phi\left(s\right)\right)^{\left(p-\delta-1\right)} \Delta^{p}g\left(s\right), \quad t \in N_{\tau+p+\delta}$$

$$\tag{4}$$

where  $p = [\delta] + 1$ , the [] is number ceiling.

If we take p=1, then the  $\delta$ -fractional difference is

$${}^{C}\Delta_{\tau}^{\delta}g\left(t\right) = \frac{1}{\Gamma\left(1-\delta\right)} \sum_{s=\tau}^{t-\left(1-\delta\right)} \left(t-\Phi\left(s\right)\right)^{\left(-\delta\right)} \Delta g\left(s\right), \quad t \in N_{\tau+1+\delta}$$
 (5)

**Theorem 2.4** [13] The following equations are equivalent

$$\begin{cases} {}^{C}\Delta_{\tau}^{\delta}(g)t = \Phi \mid t + \delta - 1, g(t + \delta - 1) \\ \Delta^{(k)}g(\tau) = g\tau, k = 0, 1, 2, ..., p - 1 \end{cases}$$
(6)

And

$$g(t) = g_0(t) + \frac{1}{\Gamma(\delta)} \sum_{s=\tau+m-\delta}^{t-\delta} \left(t - \left(\eta(s)\right)^{\delta-1}\right) \Phi\left(s + \delta - 1, g\left(s + \delta - 1\right)\right), \quad t \in N_{\tau+p}$$
 (7)

Where,  $p = [\delta] + 1$ , and

$$u_{0}(t) = \sum_{k=0}^{p-1} \frac{(t-\tau)^{(k)}}{\Gamma(k+1)} \Delta^{(k)} g(\tau)$$
 (8)

**Remark 2.5** [12] If we take  $\tau = 0$  (initial point), and  $0 < \delta < 1$ , equation (8) becomes

$$g(t) = g_0(t) + \frac{1}{\Gamma(\delta)} \sum_{s=1-\delta}^{t-\delta} \left[ (t - \tau(s))^{(\delta-1)} \Phi(s + \delta - 1, g(s + \delta - 1)) \right]$$

$$\tag{9}$$

If we use the expansion  $(t-\tau(s))^{(s-1)} = \frac{\Gamma(t-s)}{\Gamma(t-s+1-\delta)}$  and  $j=s+\delta$ , we have

$$g(t) = g_0(t) + \frac{1}{\Gamma(\delta)} \sum_{j=1}^{t} \frac{\Gamma(t-j+\delta)}{\Gamma(t-j+1)} \Phi(j-1, g(j-1))$$
(10)

#### 3. System Description

Our work is interested to investigate the dynamics and chaos of fractional order system based on the standard form:

$$x_{j+1} = x_j + \alpha \left( x_j^4 + y_j^4 - 1 \right)$$
  

$$y_{j+1} = y_j - \beta y_j \left( x_j^4 + y_j^4 - 1 \right)$$
(11)

where  $\alpha$  and  $\beta$  are real-value parameters. Based on equation (11), we construct a new system has chaotic behavior by using  $(\gamma_1, \gamma_2)$  – Caputo fractional as

$${}^{C}\Delta_{\tau}^{\gamma_{1}}x(t) = \alpha \left\{ \left( x \left( t - 1 + \gamma_{1} \right) \right)^{4} + \left( y \left( t - 1 + \gamma_{1} \right) \right)^{4} - 1 \right) \right\}$$

$${}^{C}\Delta_{\tau}^{\gamma_{2}}y(t) = -\beta \ y(t - 1 + \gamma_{2})(x(t - 1 + \gamma_{2}))^{4} + (y(t - 1 + \gamma_{2}))^{4} - 1 \right\}$$

$$(12)$$

Where  $0 < \gamma_1, \gamma_2 < 1$  are fractional orders. Now, we use theorem 1. to get on the following equivalent integral equations of system(12),

$$x(t) = x(\tau) + \frac{\alpha}{\Gamma(\gamma_{1})} \sum_{j=\tau+1}^{t} (t - \tau(j - \gamma_{1}))^{(\gamma_{1}-1)} ((x(j-1))^{4} + (y(j-1))^{4} - 1)$$

$$y(t) = y(\tau) - \frac{\beta}{\Gamma(\gamma_{2})} \sum_{j=\tau+1}^{t} (t - \tau(j - \gamma_{1}))^{(\gamma_{2}-1)} y(j-1) ((x(j-1))^{4} + (y(j-1))^{4} - 1)$$
(13)

For each , i=1,2 and  $\tau=0$  by replacing the form  $\left(t-\tau\left(j-\gamma_i\right)\right)^{(\gamma_i-1)}$  by  $\frac{\Gamma\left(t-j+\gamma_i\right)}{\Gamma\left(t-j+1\right)}$ , we obtain

$$x(t) = x_{0} + \frac{\alpha}{\Gamma(\gamma_{1})} \sum_{j=1}^{t} \frac{\Gamma(t-j+\gamma_{1})}{\Gamma(t-j+1)} \left( \left( x(j-1) \right)^{4} + \left( y(j-1) \right)^{4} - 1 \right)$$

$$y(t) = y_{0} - \frac{\beta}{\Gamma(\gamma_{2})} \sum_{j=b+1}^{t} \frac{\Gamma(t-j+\gamma_{2})}{\Gamma(t-j+1)} y(j-1) \left( \left( x(j-1) \right)^{4} + \left( y(j-1) \right)^{4} - 1 \right)$$
(14)

Where  $(x_0, y_0)$  is an initial vector.

#### 4. Visualization and Analysis

Chaotic Dynamics: In this section, we have the formula (14) to calculate the solutions of fractional chaotic system (12). We investigate the sensitivity of the fractional-order system (12) with respect to the bifurcation parameters  $\alpha$  and  $\beta$  and largest Lyapunov exponents. As seen in Figure 1., the graphs of phase portrait of the fractional dynamical system (12) with  $\alpha = 0.8$ ,  $\beta = 0.8$  and initial conditions  $x_0 = 0.81$ ,  $y_0 = -0.14$  for different values of the fractional orders  $\gamma_1$  and  $\gamma_2$  show that the trajectories x(t), y(t) are bounded when the fractional orders  $\gamma_1$  and  $\gamma_2$  are decreasing. We notice the clarity of the effect of the values of fractional orders  $\gamma_1$  and  $\gamma_2$  on the chaotic behaviour of system (12).

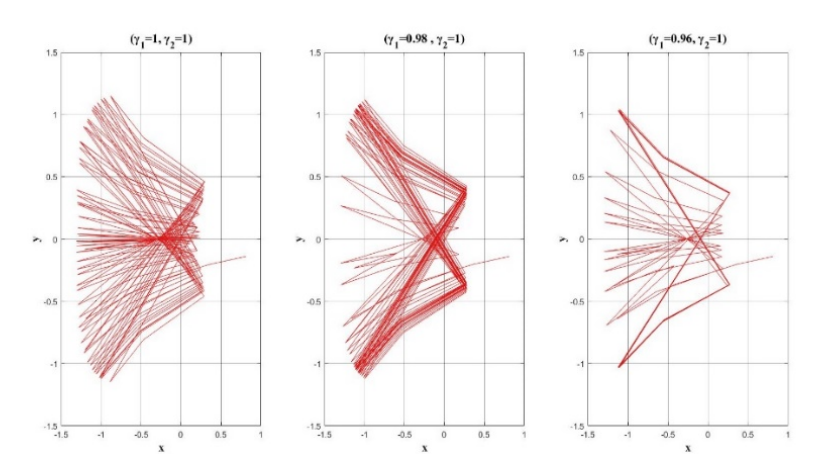


Figure 1: The chaotic attractor of proposed system in (12) with  $\alpha = 0.8$ ,  $\beta = 0.8$ ,  $x_0 = 0.81$ ,  $y_0 = -0.14$  and  $y_2 = 1$  for various fractional orders  $y_1$ .

whereas when  $\gamma_1 = 0.96$  and  $\gamma_2 = 1$ , the chaotic behavior delayed. Now, if we take the parameters  $\alpha = 0.78$ ,  $\beta = 0.78$ ,  $x_0 = 0.81$ ,  $y_0 = -0.14$  and  $\gamma_2 = 1$  of system (12), then in Figure 2. we carefully note that the effect of  $\gamma_1$  on the chaotic behavior of system (12). whereas when  $\gamma_1 = 0.96$  and  $\gamma_2 = 1$ , the chaotic behaviour delayed and the states of proposed system diverge to infinity. Also, we observe that when  $1 \le \gamma_1 \le 0.96$  the fractional dynamical system (12) exhibits a chaotic behaviour, and when  $\gamma_1 = 0.95$ , we fall in to an unbounded attractor.

Bifurcation diagrams are analyzed by varying one parameter at a time and keeping others fixed. As a first step,the parameter  $\beta=0.8$  is fixed in Figure 3 to vary  $\alpha$  along interval [0.1,0.9] with initial condition  $x_0=0.81,\ y_0=-0.14$ . The bifurcation diagrams obtained with the parameter  $\beta=0.78$  and vary  $\alpha$  along interval [0.1,0.9] with initial condition  $x_0=0.81,\ y_0=-0.14$ . Finally, in Figure 4 the bifurcation diagrams obtained with the parameter  $\alpha=0.8$  and vary  $\beta$  along interval [0.1,0.9] with initial condition  $x_0=0.81, y_0=-0.14$ . By comparing Figure 3 and Figure 4, we determine that the range where chaos exists shrinks as  $\gamma_1$  and  $\beta$  decreases. From this we conclude that a slight change of fractional order  $\gamma_1$  has a significant impact on the chaotic behavior

In figure 5, we display the time evolution of the system states corresponding to equation (12) under varying parameters and fractional orders. The largest Lyapunov exponent is one of important tools to describe the chaotic motion of a linear oand nonlinear dynamical systems. Figure 6a shows that the

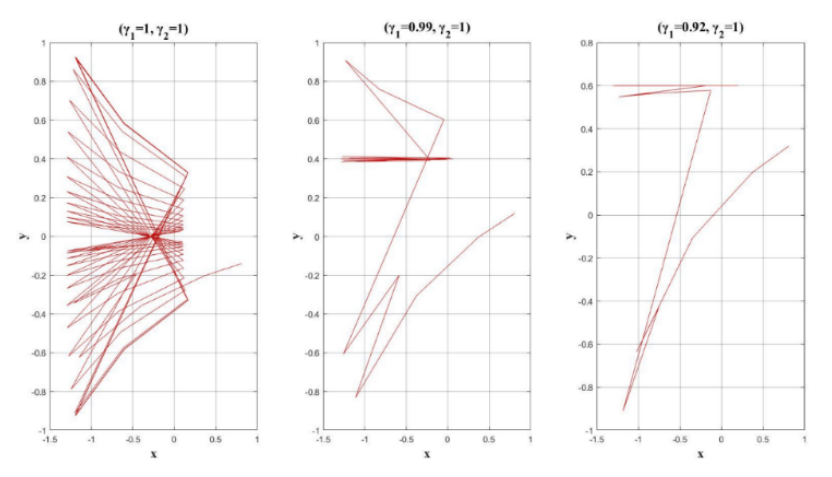


Figure 2: The chaotic attractor of proposed system in (12) with  $\alpha=0.78$ ,  $\beta=0.78$ ,  $x_0=0.81$ ,  $y_0=-0.14$  and  $\gamma_2=1$  for various fractional orders  $\gamma_1$ .

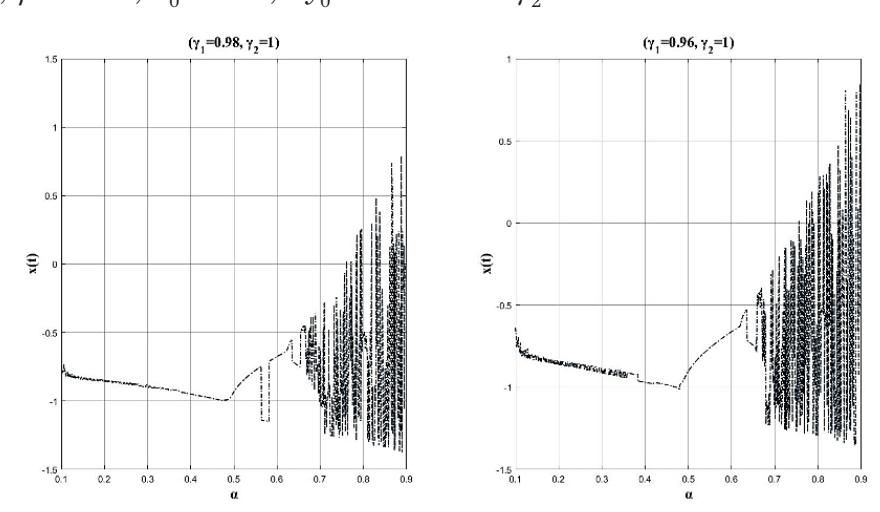


Figure 3: The bifurcation diagram of fractional chaotic system (12) on varying  $\alpha$  from 0.1 to 0.9. The other parameter is fixed  $\beta=0.8$ . For every value of  $\alpha\in [0.1,0.9]$ , we start at an arbitrary initial condition  $x_0=0.81$ ,  $y_0=-0.14$  and calculate x(t), t=1,2,...,N for N arbitrarily large.

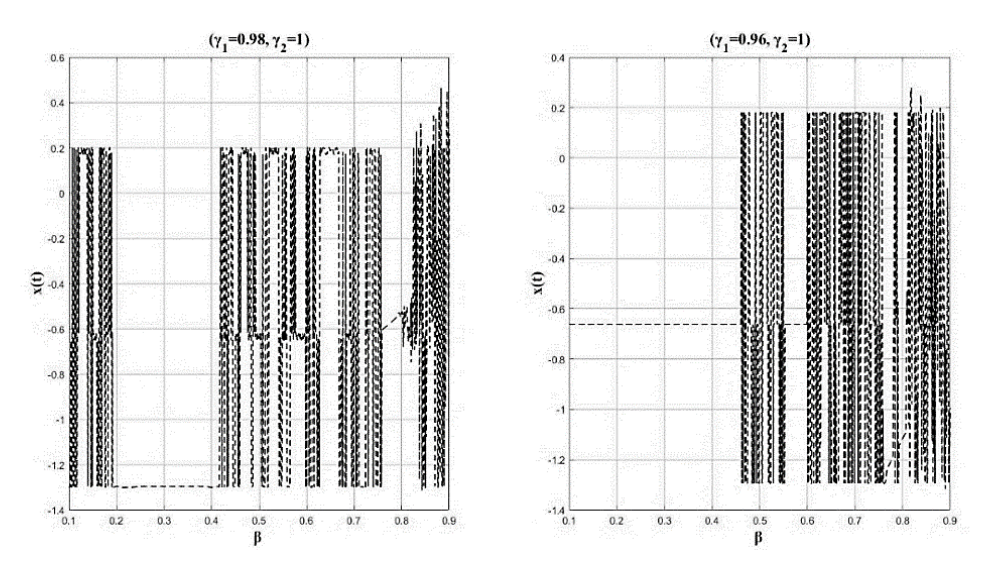


Figure 4: The bifurcation diagram of fractional chaotic system (12) on varying  $\beta$  from 0.1 to 0.9. The other parameter is fixed  $\alpha = 0.8$ . For every value of  $\beta \in [0.1, 0.9]$ , we start at an arbitrary initial condition  $x_0 = 0.81$ ,  $y_0 = -0.14$  and calculate x(t), t = 1, 2, ..., N for N arbitrarily large.

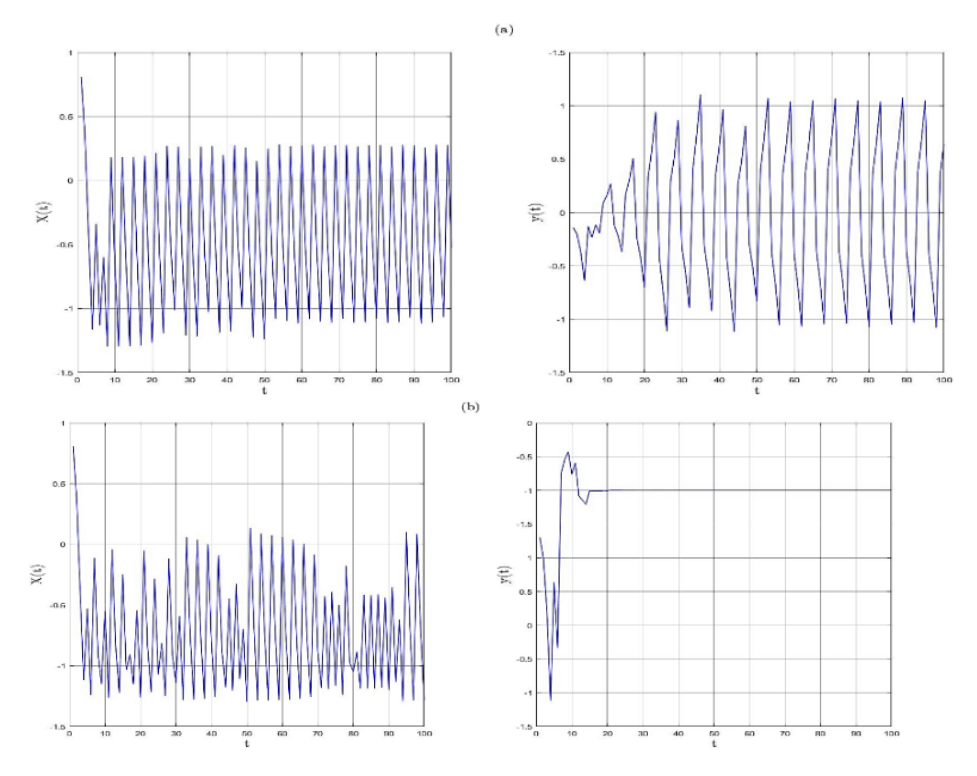


Figure 5: Time evolution of states for fractional orders  $\gamma_1=0.98, \quad \gamma_2=1$  and initial state  $x_0=0.81, \quad y_0=-0.14$  with the following parameters : (a)  $\alpha=0.8, \ \beta=0.8$  (b)  $\alpha=0.78, \ \beta=0.78$  ).

largest Lyapunov exponent of proposed system (12) with  $\beta=0.8$ , fractional orders  $\gamma_1=0.98$ ,  $\gamma_2=1$  and initial state  $x_0=0.81$ ,  $y_0=-0.14$  along to  $\alpha\in \left[0.1,0.9\right]$  is negative only if  $0.44\leq \alpha\leq 0.61$ ,  $0.7884\leq \alpha\leq 0.7912$ , and  $0.63\leq \alpha\leq 0.66$ . Therefore, the system does not show chaotic behavior but the another intervals of  $\alpha$  the largest Lyapunov exponent is positive. In Figure 6. (b) we note that the largest Lyapunov exponent of system (12) with fix  $\alpha=0.8$ , fractional orders  $\gamma_1=0.98$ ,  $\gamma_2=1$  and initial state  $x_0=0.81$ ,  $y_0=-0.14$  along to  $\beta\in \left[0.1,0.9\right]$  is always positive this means that the system is chaotic for each values of  $\beta\in \left[0.1,0.9\right]$ .

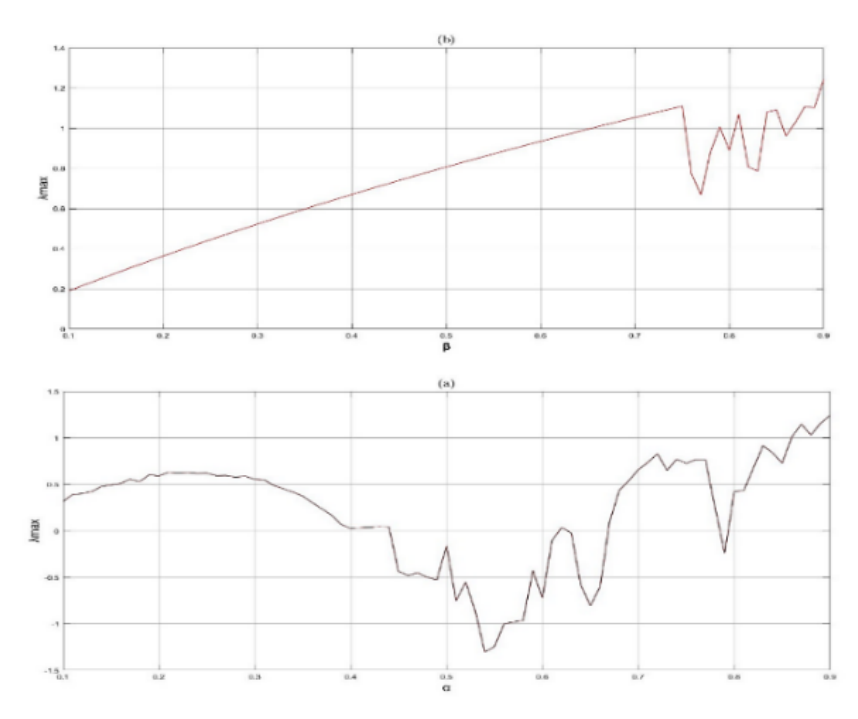


Figure 6: Evolutions of largest Lyapunov exponent  $(\lambda_{\text{max}})$  for fractional orders  $\gamma_1 = 0.98$ ,  $\gamma_2 = 1$  and initial state  $x_0 = 0.81$ ,  $y_0 = -0.14$  with the following parameters: (a)  $\beta = 0.8$  (b)  $\alpha = 0.8$ 

#### Information Analysis:

Entropy is one of helpful and applied measurement to discover various chaotic systems. Shannon C. E. (1948) [21] presented measure to quantify the uncertainty of a discrete random variable X and probability function  $f(x;\theta)$  by [22]

$$H(X;\theta) = -E(\ln(f(x;\theta)))$$
(15)

On the other hand, The Kolmogorov Sinai entropy (KS entropy), is one of the most important measures of chaotic motion of an arbitrary dimensional phase space. The KS entropy can be seen as a value measuring the creation of information at each iteration under the action of a chaotic system. In general, as the chaotic orbit evolves, the entropy provides a measure of the information gained or lost within the system. Another interpretation is that a positive value of Kolmogorov-Sinai (KS) entropy indicates the presence of chaos or disorder within the system, whereas a value of zero signifies a non-chaotic or orderly system. KS entropy is the supremum of Shannon's entropy. Calculating exact entropy of nonlinear dynamical systems is almost impossible, so we resort to approximation. The approximate entropy was proposed by Pincus [19] to present the complexity of time series. Let m be a fixed positive integer number. N data points  $\{u_n\}$  given by the vector sequences  $U_1$  through  $U_{N-m+1}$  which defined by  $U_i = (u_i, u_{i+1}, \dots, u_{i+m-1})$ . The distance between the vectors  $U_i$  and  $U_j$  is defined as  $d(U_i, U_j) = \max_{0 \le n \le m-1} |u_{n+i} - u_{n+j}|$ 

$$C_i^m(r) = \frac{\left\{number\ of\ j \le N - m + 1, d\left(U_i, U_j\right) \le r\right\}}{N - m + 1}$$

$$\tag{16}$$

Where, r is effectively a filter, also, define

$$\psi^{m}(r) = (N - m + 1)^{-1} \sum_{i=1}^{N-m+1} \ln(C_{i}^{m}(r))$$
(17)

The approximate entropy is given [20]

$$AE(r) = \psi^{m}(r) - \psi^{m+1}(r)$$
(18)

[23] showed the formula that explains the relationship between KS entropy (KSE) and Lyapunov exponents as follows,

$$KSE = \sum_{\lambda_i > 0} \lambda_i \tag{19}$$

Where,  $\lambda_i$  represent Lyapunov exponents. As entropy evolves over time, it plays a crucial role in dynamical systems by determining whether a trajectory follows a regular or irregular pattern. [24].

Figure 7 shows that in the periods,  $0.45 \le \alpha \le 0.6$ ,  $0.62 \le \alpha \le 0.66$  and  $\alpha = 0.5$ , the approximate entropy converges to zero this means that the system non-chaotic or the chaotic behavior of system almost disappeard. By comparing Figure 7. and Figure 8, we conclude that the sensitivity of the system (12) to parameter  $\alpha$  is more than to  $\beta$ . In addition, As illustrated in Figure 7 and Figure 8, when closely spaced fractional orders are considered, the entropy measures change noticeably, indicating the system's high sensitivity to fractional orders. This sensitivity is reflected in the Lyapunov exponents, which vary with the order and reveal transitions between periodic and chaotic regimes, as well as in the bifurcation diagrams that show clear qualitative shifts. Certain fractional orders make chaos more pronounced, yielding higher entropy values and larger positive Lyapunov exponents. This property highlights the richer dynamics of fractional-order systems and provides a powerful cryptography key space. content...

By Figure 9. and Table 1. can be clearly seen, that there is a loss of information in the same period in which chaos appears according to Lyapunov measure, therefore we see the boundedness relation clearly in this Figure. We observe that in the interval,  $0.5 \le \alpha \le 0.62$ , the approximate entropy converges to zero and the values of largest Lyapunov exponent are negative this means that the system non-chaotic or the chaotic behaviour of system almost disappeared. But if the values of largest Lyapunov exponent are positive, there is an increase in approximate entropy. Consequently, the entropy can be used as effective tool to explain the chaotic range of proposed system.

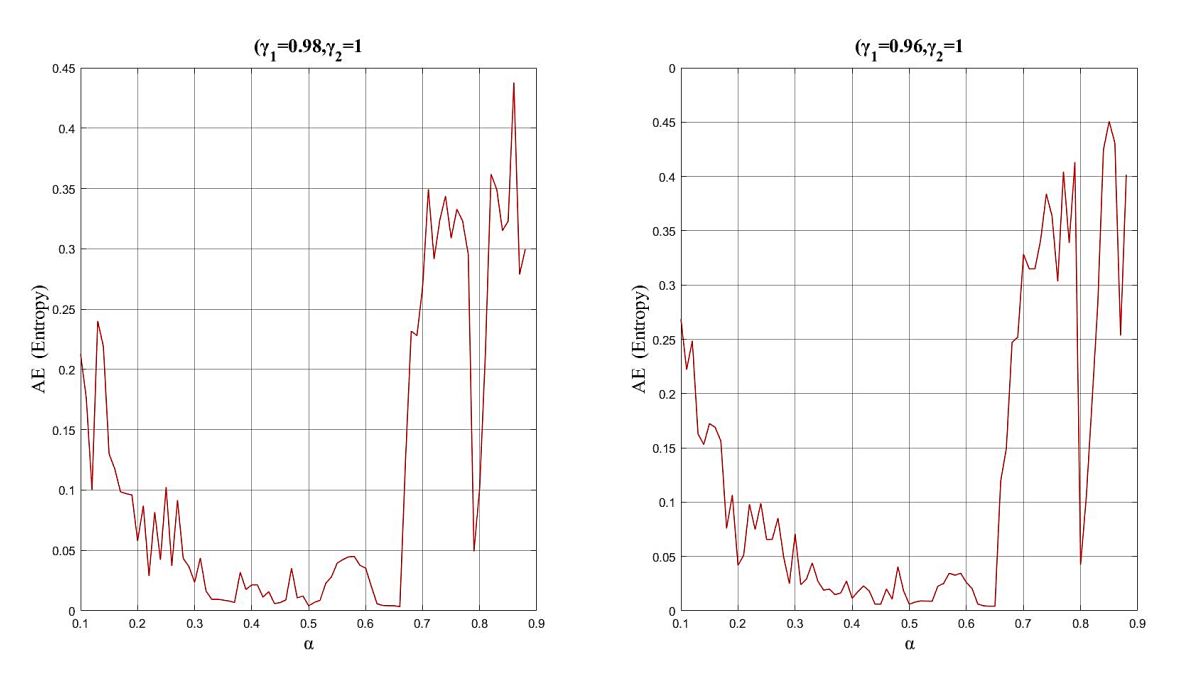


Figure 7: Evolutions of approximate entropy (AE) varying as  $\alpha \in [0.1, 0.9]$  when  $\beta = 0.8$  and the initial state  $x_0 = 0.81$ ,  $y_0 = -0.14$  with various fractional orders.

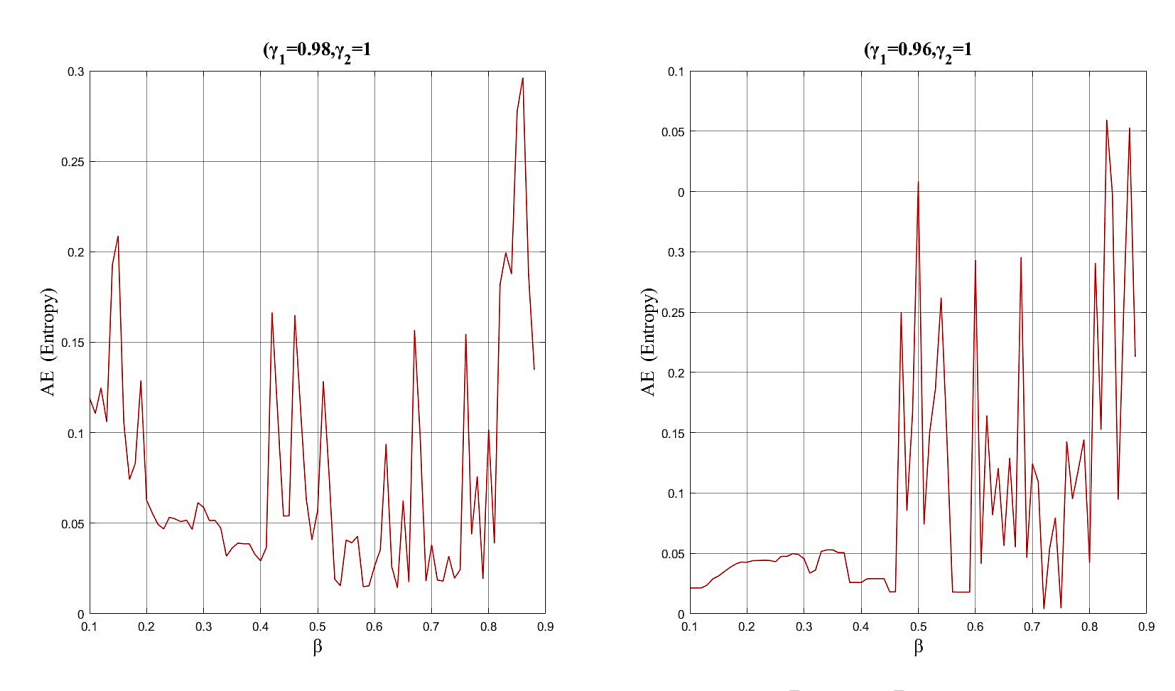


Figure 8: Evolution of approximate entropy (AE) varying as  $\beta \in [0.1, 0.9]$  when  $\alpha = 0.8$  and the initial state  $x_0 = 0.81$ ,  $y_0 = -0.14$  with various fractional orders.

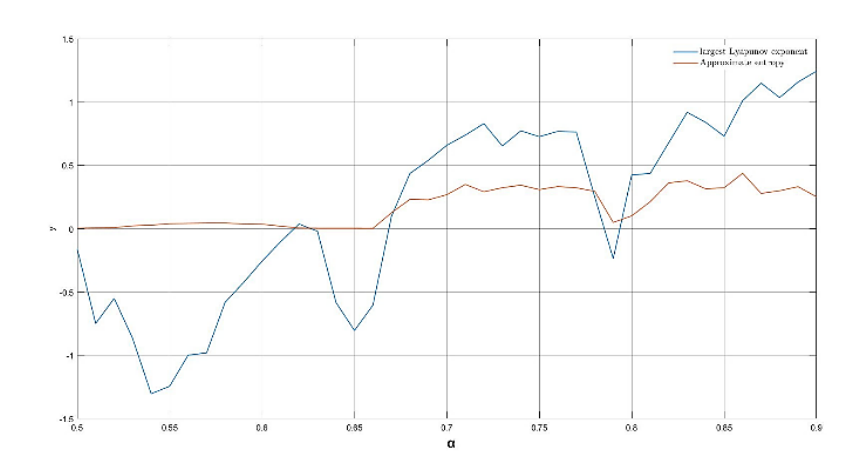


Figure 9: shows the relationship between approximate entropy (AE) and largest Lyapunov exponent  $(\lambda_{\max})$  varying as  $\alpha \in [0.5, 0.9]$  when  $\beta = 0.8$  and the initial state  $x_0 = 0.81$ ,  $y_0 = -0.14$  with fractional orders  $\gamma_2 = 1$  and  $\gamma_1 = 0.98$ .

Table 1: Calculation  $x^2$  of original and cipher images at  $\alpha=0.78, \beta=0.8$  and initial states  $x_0=0.81, y_0=-0.14$  with Fractional orders:  $\gamma_1=1, \gamma_2=0.911$ 

$x^2$			
Image	Original Image	Cipher Image	
Lena	42887	212.15	
Barbara	43001.63	241.97	
Baboon	57895.38	214.31	

#### 5. Image Encryption Application

Design and Development of the Proposed Algorithm: Chaotic dynamical systems are characterized by their distinctive and unique properties, such as extreme sensitivity to initial conditions and the non-repetitive nature of their states. This results in an inherent unpredictability, structural complexity, and a homogeneous distribution of states, making it exceedingly difficult to forecast their outcomes. Consequently, employing such systems in image encryption ensures exceptionally high levels of security. It is well understood that the connection between pixels and the elements of the image matrix is both strong and crucial. Therefore, disrupting this connection can lead to the loss of vital information contained within the image. Firstly, we produce the shuffling array  $SF_{\mathcal{R}}^{rc}$  as follows 1) (Rows shuffling) we utilize the logistic map  $a_{l+1} = ra_l \left(1 - a_l\right)$  to generate a sequence of values  $i_1, i_2, \ldots, i_m$  ensuring that  $i_k \neq i_s$  for all  $k \neq s$ . The rows of the position array  $\mathcal{R}$  are then rearranged according to these values. As a result, we obtain a newly shuffled array  $SF_{\mathcal{R}}^r$  creating a distinct pattern akin to fogbows

$$SF^r_{\mathcal{R}} = egin{bmatrix} \mathcal{R}_{i_1,1} & \mathcal{R}_{i_1,2} & \dots & \mathcal{R}_{i_1,n} \ \mathcal{R}_{i_2,1} & \mathcal{R}_{i_2,2} & \dots & \mathcal{R}_{i_2,n} \ dots & dots & dots & dots \ \mathcal{R}_{i_m,1} & \mathcal{R}_{i_m,2} & \dots & \mathcal{R}_{i_m,n} \end{bmatrix}$$

2) (columns shuffling) we apply a similar approach to generate the sequence of values  $j_1, j_2, ..., j_n$  ensuring that  $j_k \neq j_s$  for all  $k \neq s$ . The columns of the position array  $\mathcal R$  are then are then rearranged according to these values. The matrix form in step 1 is updated accordingly

$$SF^{rc}_{\mathcal{R}} = \begin{bmatrix} \mathcal{R}_{i_1,j_1} & \mathcal{R}_{i_1,j_2} & \dots & \mathcal{R}_{i_1,j_n} \\ \mathcal{R}_{i_2,j_1} & \mathcal{R}_{i_2,j_2} & \dots & \mathcal{R}_{i_2,j_n} \\ \vdots & \vdots & \vdots & \vdots \\ \mathcal{R}_{l_m,j_1} & \mathcal{R}_{l_m,j_2} & \dots & \mathcal{R}_{l_m,j_n} \end{bmatrix}$$

The steps of proposed image encryption algorithm are outlined as follows:

**Step 1:** The original image is converted into an  $m \times n$  grayscale image denoted as  $\mathcal{R}$ .

**Step 2:** The shuffling array  $SF_{\mathcal{R}}^{rc}$  is generated.

Step 3: The values of a matrix  $SF_{\mathcal{R}}^{rc}$  are then transformed from decimal to binary, resulting in a set  $\mathcal{M} = \{\mathcal{M}_1, \mathcal{M}_2, ..., \mathcal{M}_{mn}\}$ .

Step 4: Use the formula (14) to generate the sequences  $x = \{x_1, x_2, ..., x_{mn}\}$  and  $y = \{y_1, y_2, ..., y_{mn}\}$  as

- 1. Determine the initial vector (x(1), y(1)).
- 2. For t = 2:mn; S1=0; S2=0;

For j = 1:t, compute

$$S1=S1+\frac{\Gamma(t-j+\gamma_1)}{\Gamma(t-j+1)}\Big((x(j-1))^4+(y(j-1))^4-1\Big),$$

$$S2=S2+\frac{\Gamma(t-j+\gamma_2)}{\Gamma(t-j+1)}y(j-1)\Big((x(j-1))^4+(y(j-1))^4-1\Big)$$

End

$$x(t) = x(1) + \frac{\alpha}{\Gamma(\gamma_1)}S1, \ y(t) = y(1) - \frac{\beta}{\Gamma(\gamma_2)}S2$$

End

Step 5: Rewrite the sequences  $x = \{x_1, x_2, ..., x_{mn}\}$  and  $y = \{y_1, y_2, ..., y_{mn}\}$  and obtained in step 4 as

$$x = floor(mod(x \times 10^{14}), 256)$$

$$y = floor(mod(y \times 10^{14}), 256)$$

Step 6: Transform the values obtained in step 5 from decimal to binary, resulting in binary sequences  $\mathcal{B}^{x} = \left\{ \mathcal{B}_{1}^{x}, \mathcal{B}_{1}^{x}, \dots, \mathcal{B}_{mn}^{x} \right\} \text{ and } \mathcal{B}^{y} = \left\{ \mathcal{B}_{1}^{y}, \mathcal{B}_{1}^{y}, \dots, \mathcal{B}_{mn}^{y} \right\} \text{ for x and y, respectively.}$  **Step 7:** Apply a bitwise XOR operation between  $\mathcal{B}^{x}$  and  $\mathcal{B}^{y}$ , yielding  $\mathcal{B} = bitxor(\mathcal{B}^{x}, \mathcal{B}^{y})$ .

**Step 8:** Perform a bitwise XOR operation between the original grayscale image  $\mathcal{M}$  and  $\mathcal{B}$ , resulting in  $E = bitxor(\mathcal{M}, \mathcal{B})$ .

Step 9: Transform the values of a matrix E from binary to decimal, producing the set  $D = \{D_1, D_2, \dots, D_{mn} \}.$ 

**Step 10:** Reshape the vector D to be a matrix C with dimension  $m \times n$ , representing the cipher image.

**Experimental Analysis:** In this subsection, we analyse the performance of the proposed algorithm through a series of experiments conducted on a variety of images. To evaluate its efficiency, the algorithm was tested on three standard benchmark images: Lena (256x256 pixels), Barbara (256x256 pixels), and Baboon (256x256 pixels). These images were selected due to their common use and significance in image processing research. The purpose of this analysis is to highlight the algorithm's effectiveness and robustness in practical applications. The experimental results presented in Figure 10 demonstrate that the image encryption process under investigation is both effective and reliable when compared to previous studies. The proposed fractional-order chaotic system generates a highly sensitive chaotic random sequence, particularly in relation to initial conditions and the encryption key. Any modification of these parameters leads to a significantly altered encrypted image, which enhances security and ensures robust resistance to brute-force attacks. This confirms the system's suitability for secure encryption applications. The image histogram is utilized to represent the distribution of pixels across different gray levels, illustrating the number of pixels at each intensity value. Significant statistical insights regarding the image can be extracted from its histogram. For an encrypted image, the histogram should display a uniform distribution, distinctly differing from that of the original image, indicating successful encryption. In Figure 10, the histograms corresponding to the encrypted images, displayed on the right side, reveal an almost uniform distribution of pixel intensities across all levels. This uniformity is a hallmark of encryption techniques aimed at concealing the original visual content. By distributing pixel intensities evenly, the encryption effectively eliminates the recognizable patterns found in the original images, thereby enhancing security by rendering the encrypted image visually incoherent. The comparison between the histograms of the original and encrypted images highlights the encryption process's success. The shift from a structured, recognizable pattern in the original histograms to a flat, uniform distribution in the encrypted histograms demonstrates that the encryption method has effectively disrupted the original pixel intensity distributions, ensuring that the encrypted images retain no discernible traces of the original content.

Statistical and Entropy Analysis: It is well-established that encrypted images demonstrate a uniform distribution when statistical tests, such as the Chi-square test, show that their distribution does not significantly deviate from uniformity. This is confirmed when the Chi-square test value falls below the critical value from the table, supporting the null hypothesis, which implies that the distribution closely resembles a uniform distribution.

The chi-square test [25] can be utilized to evaluate the uniformity and consistency of data distribution using the following formula

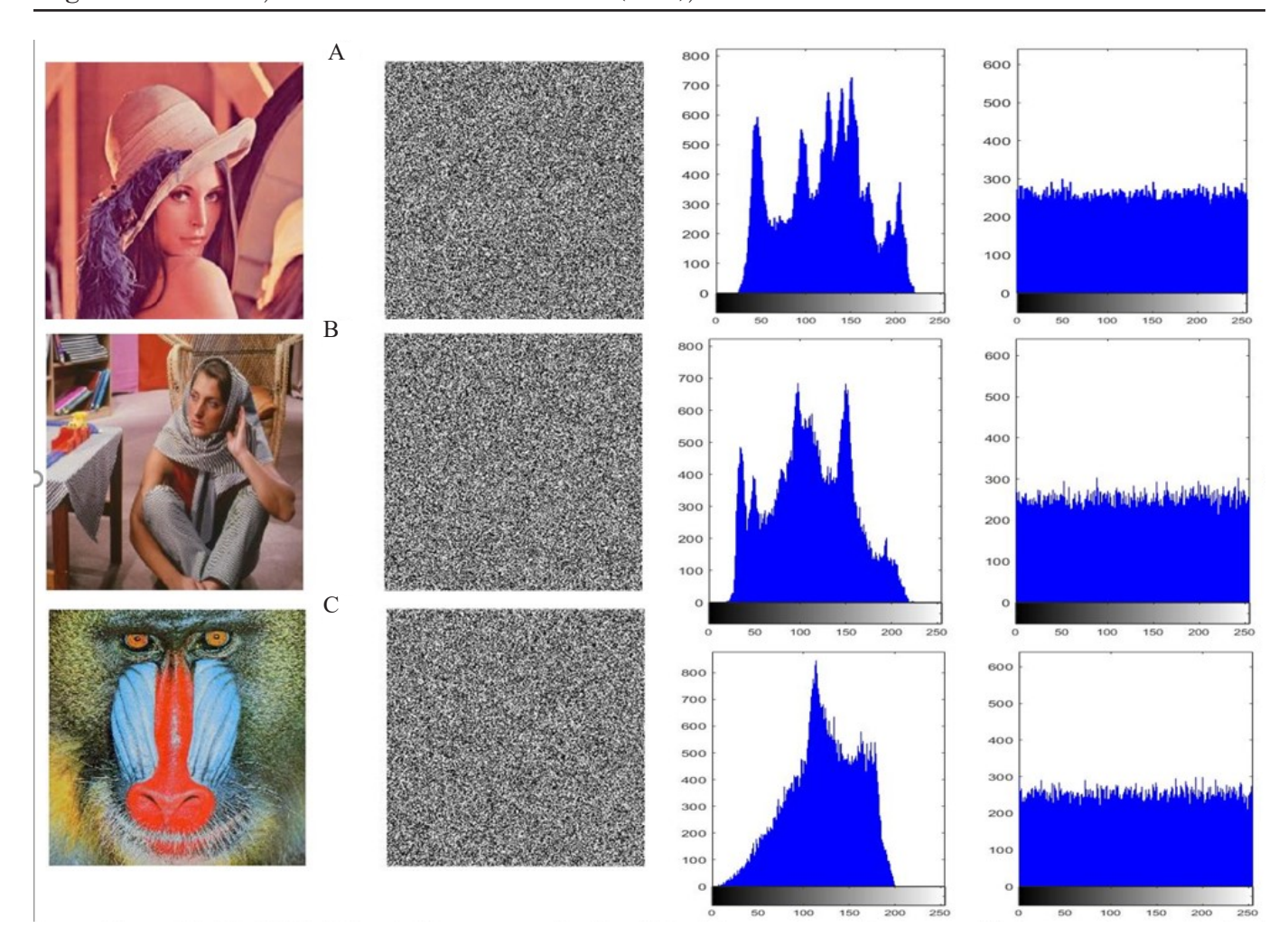


Figure 10: (Left) (A), (B) and (C) correspond to the original images Lena, Barbara and baboon and respectively along with their associated encrypted (cipher) versions. These figures illustrate the transformation of the original images into their ciphered counterparts, highlighting the effectiveness of the encryption process. (Right) (A), (B) and (C) refer to Original image and Cipher image histograms of Lena, Barbara and baboon respectively..

Table 2. Calculation Entropy of original and cipher images at  $\alpha = 0.78$ ,  $\beta = 0.8$  and initial states  $x_0 = 0.81$ ,  $y_0 = -0.14$  with Fractional orders:  $\gamma_1 = 1$ ,  $\gamma_2 = 0.911$ 

Entropy			
Image	Original Image	Cipher Image	
Lena	7.7441	7.9977	
Barbara	7.6387	7.9973	
Baboon	7.7680	7.9976	

$$x^{2} = \sum_{s=1}^{\eta} \frac{\left(M_{s} - m_{s}\right)^{2}}{m_{s}} \tag{20}$$

where,  $\eta = 256$  and  $M_s$  and  $m_s$  represent the observed and the expected occurrence frequencies of each gray level (0-255). A significance level of 0.05 is used in this test. The purpose of this test is

to measure the discrepancies between the observed and expected distributions, helping to determine whether the data conforms to an expected pattern or deviates significantly. The chi-square values for the encrypted images are provided in Table 1. It is clear that  $x^2(\eta-1,0.05)=x^2(255,0.05)=293$ . Therefore, the null hypothesis is accepted at this level of significance, indicating that the histograms of the encrypted images exhibit a uniform distribution. As presented in Table 1, the computed  $x^2$  values are less than the critical value of  $x^2(255,0.05)$ 

#### 6. Conclusion

In this study, we examined a class of discrete fractional chaotic systems. While various tools, such as Lyapunov exponents, bifurcation diagrams, and chaotic attractors, are commonly used to demonstrate chaotic behavior, we also incorporated entropy as a straightforward method to confirm chaos. Additionally, we clarified several fundamental aspects of chaos theory and entropy within the context of fractional dynamical systems. The tools of chaos theory—namely, the bifurcation diagram, Lyapunov exponents, chaotic attractors, and entropy—were shown to be effective in validating chaotic behavior in these systems. Furthermore, we highlighted the relationship between Lyapunov exponents and entropy, demonstrating their role in explaining the chaotic range of the proposed system. At first glance, the chaotic behavior of the standard form (11) may appear similar to that of classical first-order dynamical systems. However, the dynamics of the fractional-order system (12) are notably more complex due to their heightened sensitivity to fractional orders. From an applied perspective, such as in cryptography or communication systems, the fractional orders can be regarded as an important parameter, acting as a key component in the process. Our findings indicate that entropy is an effective and easily applicable measure of chaos. Additionally, the results confirm that the designed system exhibits the property of coexisting attractors. Moreover, this paper introduces a carefully developed algorithm designed for image encryption. The algorithm utilizes the logistic map to systematically shuffle the matrix elements that represent the pixels of the image being encrypted. The encryption process is then carried out using chaotic systems with fractional orders, as outlined in this study. Experimental results conducted on various images demonstrate that the proposed algorithm not only achieves high levels of efficiency but also exhibits remarkable robustness. This makes it highly resistant to cryptanalytic attacks, thus significantly enhancing the overall security of the encryption process.

Finally, we would refer to this study opens several promising directions for future work. One potential extension is to investigate fractional orders beyond the interval  $0 < \gamma \le 1$ , which may uncover richer dynamical behaviors and provide additional flexibility for encryption design. Another avenue is the generalization of the proposed system to higher dimensions, thereby increasing the complexity and security level of the encryption process. Moreover, practical aspects such as hardware implementation and real-time optimization should be explored to reduce computational cost and enhance the applicability of the proposed scheme in real-world encryption scenarios.

#### References

- [1] J. D. Markel and A. H. J. Gray, Linear prediction of speech, vol. 12. Springer Science & Business Media, 2013.
- [2] L. R. Rabiner and R. W. Schafer, Programs for supporting the teaching of digital speech processing, in 2013 IEEE Digital Signal Processing and Signal Processing Education Meeting (DSP/SPE), IEEE, 2013, pp. 290–295.
- [3] J.-H. He, A review on some new recently developed nonlinear analytical techniques, International Journal of Nonlinear Sciences and Numerical Simulation, vol. 1, no. 1, pp. 51–70, 2000.
- [4] S. H. Abid and U. J. Quaez, Capacity of control for stochastic dynamical systems perturbed by mixed fractional brownian motion with delay in control, International Journal of Innovative Computing, Information and Control, vol. 15, no. 5, pp. 1913–1934, 2019, doi: 10.24507/ijicic.15.05.1913.
- [5] M. Henon, A two-dimensonal mapping with a strange attractor, Communications in Mathematical Physics, vol. 50, pp. 376–392, 1976.
- [6] R. Lozi, Un attracteur étrange (?) du type attracteur de Hénon, Le Journal de Physique Colloques, vol. 39, no. C5, pp. C5-9, 1978.

- [7] D. L. Hitzl and F. Zele, An exploration of the Hénon quadratic map, Physica D: Nonlinear Phenomena, vol. 14, no. 3, pp. 305–326, 1985.
- [8] G. Baier and S. Sahle, "Design of hyperchaotic flows," Physical Review E, vol. 51, no. 4, p. R2712, 1995.
- [9] K. Stefański, "Modelling chaos and hyperchaos with 3-D maps," Chaos, Solitons & Fractals, vol. 9, no. 1-2, pp. 83–93, 1998.
- [10] M. Itoh, T. Yang, and L. O. Chua, Conditions for impulsive synchronization of chaotic and hyperchaotic systems, International Journal of Bifurcation and Chaos, vol. 11, no. 02, pp. 551–560, 2001
- [11] H. Zhang, D. Liu, and Z. Wang, Controlling chaos: suppression, synchronization and chaotification. Springer Science & Business Media, 2009.
- [12] A. Ouannas, X. Wang, A.-A. Khennaoui, S. Bendoukha, V.-T. Pham, and F. E. Alsaadi, Fractional form of a chaotic map without fixed points: Chaos, entropy and control," Entropy, vol. 20, no. 10, p. 720, 2018.
- [13] A.-A. Khennaoui, A. Ouannas, S. Bendoukha, X. Wang, and V.-T. Pham, On chaos in the fractional-order discrete-time unified system and its control synchronization, Entropy, vol. 20, no. 7, p. 530, 2018.
- [14] A. K. Bagheedh, S. H. Abid, and S. A. Mehdi, Design a Fractional Chaotic Logistic Dynamical System, in Journal of Physics: Conference Series, IOP Publishing, 2021, p. 12055.
- [15] J. Dambre, D. Verstraeten, B. Schrauwen, and S. Massar, Information processing capacity of dynamical systems, Scientific reports, vol. 2, no. 1, p. 514, 2012.
- [16] S. Tiomkin, D. Polani, and N. Tishby, Control capacity of partially observable dynamic systems in continuous time, arXiv preprint arXiv:1701.04984, 2017.
- [17] P. Gaspard and X.-J. Wang, Sporadicity: between periodic and chaotic dynamical behaviors, Proceedings of the National Academy of Sciences, vol. 85, no. 13, pp. 4591–4595, 1988.
- [18] G. Deco and B. Schurmann, Information flow and chaotic dynamics, in Proceedings of International Workshop on Neural Networks for Identification, Control, Robotics and Signal/Image Processing, IEEE, 1996, pp. 321–329.
- [19] S. M. Pincus, Approximate entropy as a measure of system complexity., Proceedings of the national academy of sciences, vol. 88, no. 6, pp. 2297–2301, 1991.
- [20] S. Pincus, Approximate entropy (ApEn) as a complexity measure, Chaos: An Interdisciplinary Journal of Nonlinear Science, vol. 5, no. 1, pp. 110–117, 1995.
- [21] C. E. Shannon, A mathematical theory of communication, The Bell system technical journal, vol. 27, no. 3, pp. 379–423, 1948.
- [22] S. H. Abid and U. J. Quaez, Rényi entropy for mixture model of multivariate skew Laplace distributions, in Journal of Physics: Conference Series, IOP Publishing, 2020, p. 12037.
- [23] J. B. Pesin, Ljapunov characteristic exponents and ergodic properties of smooth dynamical systems with an invariant measure, in Hamiltonian Dynamical Systems, CRC Press, 2020, pp. 512–515.
- [24] M. Mondal, F. Rahaman, and K. Singh, "Lyapunov exponent, ISCO and Kolmogorov-Senai entropy for Kerr-Kiselev black hole," The European Physical Journal C, vol. 81, no. 1, pp. 1–16, 2021.
- [25] H. S. Kwok and W. K. S. Tang, A fast image encryption system based on chaotic maps with finite precision representation, Chaos, solitons & fractals, vol. 32, no. 4, pp. 1518–1529, 2007.
- [26] U. J. Quaez, Dynamics and Entropy Analysis of a Novel Fractional Chaotic System For Color Medical Image Encryption, International Journal of Innovative Computing, Information and Control (IJICIC), vol. 21, no. 4, pp. 919–935, 2025.